

# LW-FedSSL: Resource-Efficient Layer-wise Federated Self-Supervised Learning

Ye Lin Tun<sup>1</sup>, Chu Myaet Thwal<sup>1</sup>, Le Quang Huy<sup>1</sup>, Minh N. H. Nguyen<sup>2</sup>, Choong Seon Hong<sup>1\*</sup>

<sup>1</sup> Kyung Hee University, Yongin-si, Republic of Korea  
 {yelintun, chumyaet, quanghuy69, cshong}@khu.ac.kr

<sup>2</sup> Vietnam - Korea University of Information and Communication Technology, Danang, Vietnam  
 nhnminh@vku.udn.vn

**Abstract**—Many studies integrate federated learning (FL) with self-supervised learning (SSL) to take advantage of raw training data distributed across edge devices. However, edge devices often struggle with high computation and communication costs imposed by SSL and FL algorithms. To tackle this hindrance, we propose LW-FedSSL, a layer-wise federated self-supervised learning approach that allows edge devices to incrementally train a single layer of the model at a time. Our LW-FedSSL comprises server-side calibration and representation alignment mechanisms to maintain comparable performance with end-to-end federated self-supervised learning (FedSSL) while significantly lowering clients' resource requirements. In a pure layer-wise training scheme, training one layer at a time may limit effective interaction between different layers of the model. The server-side calibration mechanism takes advantage of the resource-rich server in an FL environment to ensure smooth collaboration between different layers of the global model. During the local training process, the representation alignment mechanism encourages closeness between representations of FL local models and those of the global model, thereby preserving the layer cohesion established by server-side calibration. Our experiments show that LW-FedSSL has a  $3.3\times$  lower memory requirement and a  $3.2\times$  cheaper communication cost than its end-to-end counterpart. We also explore a progressive training strategy called Prog-FedSSL that outperforms end-to-end training with a similar memory requirement and a  $1.8\times$  cheaper communication cost.

**Index Terms**—federated learning, self-supervised learning, layer-wise training, resource-efficient.

## I. INTRODUCTION

A significant portion of real-world data, valuable for practical AI applications, resides on edge devices. Such data is often unlabeled, making the adoption of self-supervised learning (SSL) strategies [1], [2], [3] essential. SSL enables models to learn from raw data by generating their own supervisory signals, eliminating the need for labels. Most SSL methods follow centralized training schemes, often requiring an exhaustive data collection process to build a centrally stored dataset. Although some data, such as natural images, can be conveniently collected, it can raise significant concerns for privacy-sensitive data, such as medical data. Meanwhile, decentralized learning approaches like federated learning (FL) [4], [5] enables privacy-preserving collaborative model training. An FL system functions by collecting trained model

parameters from edge devices (a.k.a., clients) rather than data. This mechanism safeguards the confidentiality of private data held by different parties. As a result, federated self-supervised learning (FedSSL) approaches have recently emerged as a potential strategy for leveraging raw data in distributed environments [6], [7], [8].

Self-supervised learning (SSL), especially when involving state-of-the-art models like transformers [9], [10], can impose substantial computation demands. Unfortunately, clients in an FL environment often operate with limited computation and communication resources. Therefore, it is crucial to explore resource-efficient SSL approaches for FL systems. A straightforward way to reduce computation demands on low-memory devices is to conduct the training with a smaller batch size. However, using a small batch size for SSL approaches can diminish the quality of learned representations and compromise performance [1], [7]. Moreover, simply reducing the batch size does not lower the FL communication cost since clients still need to exchange the full model with the server. On the other hand, using a large batch size would exclude low-memory devices from participating in the FL process.

One promising solution is the layer-wise training approach, where a model is systematically trained one layer at a time, gradually increasing its depth. The term “layer” can refer to either an individual layer or a block comprising multiple layers. In layer-wise training, only a single layer is active at a time for training, significantly reducing computation requirements on FL clients. Moreover, only the active layer needs to be exchanged with the server, further reducing communication costs. Table I shows a significant reduction in a client's resource requirements for layer-wise training compared to end-to-end training.

Although layer-wise training significantly reduces resource requirements, it may not be able to match the performance of end-to-end training as shown in Table I. In each stage of layer-wise training, a new layer is sequentially attached to the model, and all preceding layers are frozen, excluding them from further updates. Given a fixed number of FL rounds for each stage, it can be challenging to train the newly added layer to work seamlessly with the previous layers, especially if the number of rounds is small. Although increasing the number of rounds could potentially alleviate this problem, it would

TABLE I: FedMoCo (end-to-end) vs. LW-FedMoCo (layer-wise). We use a ViT-Tiny backbone with MoCo v3 as the SSL approach. The FL process involves 10 clients using a batch size of 1024 and the number of communication rounds set to 180. The unlabeled portion of STL-10 dataset is used to setup the clients' data, while the labeled training and testing portions are used for linear evaluation. We compare resource requirements for a single client.

	Memory (MB)	Comm. (MB)	Accuracy (%)
<b>FedMoCo</b>	15601	7352.49	54.99
<b>LW-FedMoCo</b>	3927	613.19	46.41

impose extra communication and computation overhead on the clients, canceling the benefits of layer-wise training.

To address these challenges, we propose LW-FedSSL, by introducing two simple, yet effective mechanisms: *server-side calibration* and *representation alignment*. Although clients in an FL environment may have limited resources, the central server typically possesses significant computation power. Therefore, in LW-FedSSL, the server-side calibration mechanism leverages the computation resources of the central server to train the global model in an end-to-end manner using an auxiliary dataset. This mechanism solely operates on the central server and incurs no additional overhead on the clients. Meanwhile, the representation alignment mechanism encourages alignment between local models and the server-side-trained global model during the local training process.

Our contributions can be summarized as follows: (i) We conduct an in-depth exploration of layer-wise training for FedSSL, considering various empirical aspects. (ii) We introduce LW-FedSSL, a novel layer-wise training framework designed to improve the resource efficiency of SSL within the FL paradigm. LW-FedSSL can compete with conventional end-to-end training while significantly lowering the resource requirements of FL clients. (iii) We also explore a progressive training approach called Prog-FedSSL. Although the progressive approach requires more resources than the layer-wise approach, it still remains more resource-efficient than end-to-end training while significantly outperforming both.

## II. PRELIMINARY

In this section, we present fundamental concepts related to federated learning and self-supervised learning.

### A. Federated Learning

A typical FL [5] process involves a central coordinating server and a set of client devices, each of which stores private data. The goal of FL is to train a global model  $M$ , by learning from the data residing on clients while ensuring their privacy. The FL objective can be expressed as

$$M^* = \arg \min_M \sum_{i=1}^N w^i \mathcal{L}(M, D^i), \quad (1)$$

where  $N$  is the number of clients and  $\mathcal{L}$  is the local loss. Here,  $w^i = |D^i|/|D|$ , which is the weight term of  $i$ -th client, with

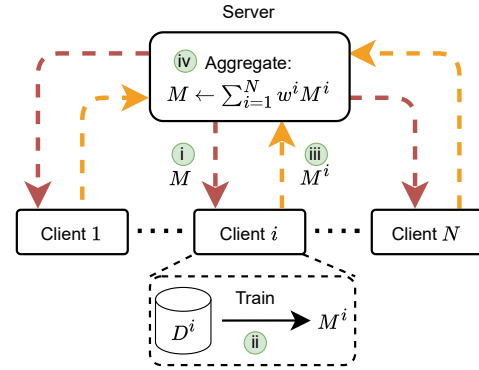


Fig. 1: Four key steps in an FL communication round.

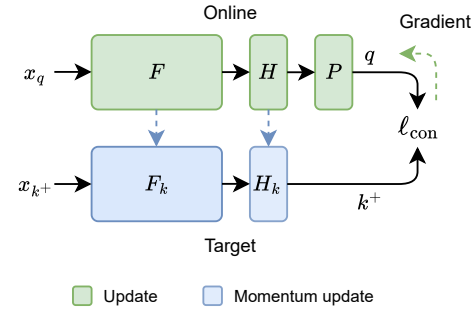


Fig. 2: Self-supervised learning with MoCo v3. We omit the negative samples for clarity.

$|D^i|$  denoting the number of samples in local dataset  $D^i$  and  $|D|$  denoting the total number of samples in  $D = \bigcup_{i=1}^N D^i$ . As shown in Fig. 1, a single FL communication round consists of the following four key steps. At the beginning of each round, (i) the server distributes a base global model  $M$  to all participating clients. (ii) Each client  $i \in [1, N]$  performs training on its local dataset  $D^i$  to produce a local model  $M^i$ . After the training, (iii) local models are transmitted back to the server. Finally, (iv) the sever aggregates the received local models through weighted averaging [5] to update the global model:  $M \leftarrow \sum_{i=1}^N w^i M^i$ . These four steps are repeated for a number of rounds  $R$ .

### B. Self-Supervised Learning

Self-supervised learning (SSL) offers a means to utilize unlabeled data, which is often more readily available than labeled data, for model training. SSL generates its own supervisory signals to learn valuable representations from the unlabeled data. We select MoCo v3 [11] as the SSL approach in our work. As shown in Fig 2, MoCo v3 features a Siamese network structure with an actively trained online branch, and a target branch, which is a moving-averaged copy of the online branch. The online branch consists of an encoder  $F$ , a projection head  $H$ , and a prediction head  $P$ . Meanwhile, the target branch consists of a momentum encoder  $F_k$  and a momentum projection head  $H_k$ . Given an input sample  $x$ , it undergoes augmentation, creating two views,  $x_q$  and  $x_{k+}$ . These views are then fed into the online and target branches, respectively, to obtain a vector  $q$  and its corresponding positive

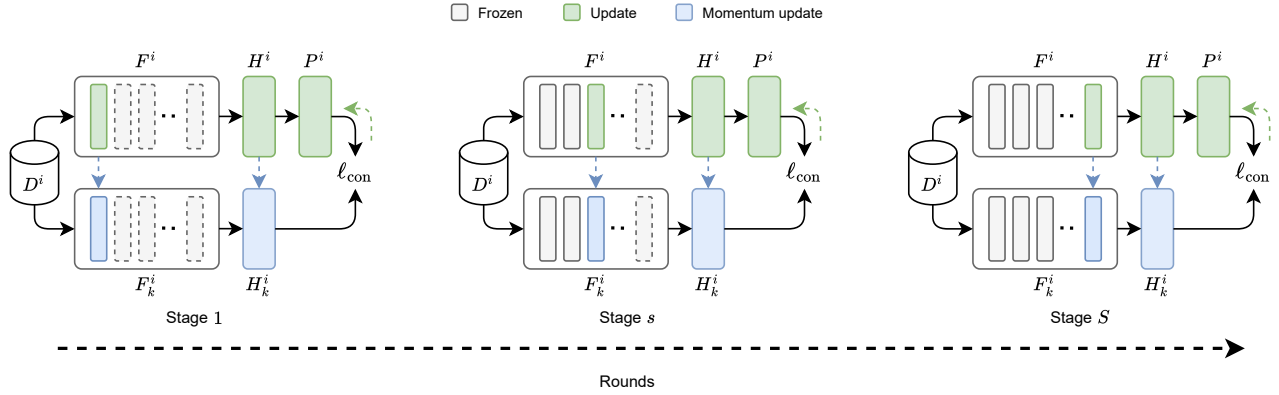


Fig. 3: Local training process of LW-FedMoCo across different stages for  $i$ -th client. Each stage  $s \in [1, S]$  increases the depth of the encoder  $F$  by adding a new layer  $L_s$ . During stage  $s$ , only the corresponding layer  $L_s$  is actively updated, while prior layers (i.e.  $L_1$  to  $L_{s-1}$ ) are frozen.

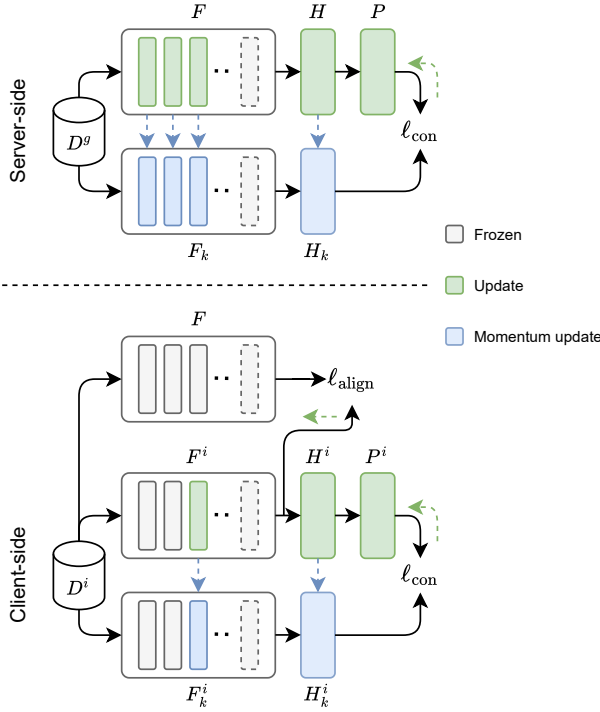


Fig. 4: LW-FedSSL at stage  $s$ . The server-side calibration mechanism (top) trains all existing layers in the current sub-model. The representation alignment mechanism (bottom) aligns the representations of the local model with those of the global model during the local training process.

pair,  $k^+$ . Likewise, negative pairs,  $k^-$ , are derived from other samples within the same batch through the target branch. The online branch is trained using the InfoNCE loss [12],

$$\ell(q, k, \tau) = -\log \frac{\exp(q \cdot k^+ / \tau)}{\exp(q \cdot k^+ / \tau) + \sum_{j=1}^K \exp(q \cdot k_j^- / \tau)}, \quad (2)$$

where  $k = (k^+, \{k_j^-\}_{j=1}^K)$  and  $\tau$  is the temperature parameter. Using a momentum parameter  $\mu$ , the target branch is updated as:  $F_k \leftarrow \mu F_k + (1 - \mu)F$  and  $H_k \leftarrow \mu H_k + (1 - \mu)H$ .

### C. Federated Self-Supervised Learning

Although numerous studies on FL primarily focus on supervised learning, this means that device owners are tasked with labeling data, which is a tedious process. Consequently, client devices often lack labeled data due to various reasons, including limitations in data collection methods, labeling constraints, and insufficient annotation expertise and resources. In response, federated self-supervised learning (FedSSL) [13], [14], [15] emerges as a solution to extend the applicability of FL to new applications and use cases in domains where labeled data is scarce or difficult to acquire. Therefore, in the context of FedSSL, the local dataset  $D^i$  within a client  $i$  is unlabeled, and thus, the local training process involves utilizing a form of SSL loss to train the local model  $M^i$  on  $D^i$ . When using MoCo v3 as the SSL approach, this local model can comprise an encoder  $F^i$  and its accompanying MLP heads,  $H^i$  and  $P^i$ .

### III. RELATED WORK

Layer-wise training was initially introduced in the context of deep belief networks and restricted Boltzmann machines [16], [17]. The original motivation behind its development was to address the challenges associated with training deep neural networks, such as vanishing gradients. While layer-wise training has become less common over the years, it can still be effectively employed as a resource-efficient strategy within FL systems. Training the model incrementally, one layer at a time, offers a distinct resource-saving advantage over end-to-end training. To date, only a very limited number of studies [18], [19] have explored layer-wise training in the FL context, and even fewer [19] have examined its application in the domain of FedSSL.

Some studies [20], [21] reduce computation costs of FL clients by selectively dropping parts of the model. Federated Dropout [20] randomly removes a subset of neurons or filters from a layer to reduce the computation cost while relying on compression techniques to minimize the communication overhead. FjORD [21], a similar approach, introduces an ordered dropout mechanism instead of random dropping. Meanwhile, [18] proposes a progressive training approach for FL called ProgFed. While similar to layer-wise training

**Algorithm 1** LW-FedSSL (*Server-side*)

---

**Input:** encoder  $F$ , projection head  $H$ , prediction head  $P$ , auxiliary dataset  $D^g$ , number of epochs  $E$ , momentum  $\mu$ , temperature  $\tau$ , number of stages  $S$ , number of rounds per stage  $R_s$ ,  $R \leftarrow \sum_{s=1}^S R_s$   
**Output:** encoder  $F$

- 1: **Server executes:**
- 2: Initialize stage:  $s = 0$
- 3: **for** round  $r = 1, 2, \dots, R$  **do**
- 4:   **if**  $r > \sum_{j=1}^s R_j$  **then**
- 5:      $s \leftarrow s + 1$
- 6:     Append a new layer  $L_s$  to  $F$
- 7:     Unfreeze  $F$
- 8:      $F, H, P \leftarrow \text{Server\_SSL}(D^g, E, \mu, \tau, F, H, P)$
- 9:     Freeze  $F$  up to layer  $L_{s-1}$
- 10:   **for** client  $i = 1, 2, \dots, N$  in parallel **do**
- 11:      $L_s^i, H^i, P^i \leftarrow \text{Local\_SSL}(i, F, H, P)$       Algo. 2
- 12:      $w^i = \frac{|D^i|}{|D|}$ , where  $D = \bigcup_{i=1}^N D^i$
- 13:      $L_s, H, P \leftarrow \text{Aggregation}(\{L_s^i, H^i, P^i, w^i\}_{i=1}^N)$
- 14:     Update  $L_s$  in  $F$
- 15: **return**  $F$

---

in gradually increasing the model depth, ProgFed differs by training all existing layers at each stage. All aforementioned studies primarily focus on federated supervised learning tasks that require labeled data for training.

On the other hand, [22] studies layer-wise SSL in the speech domain. While the study was intended for an on-device training scenario, the authors mainly examined it in a centralized setting. Another study in [19] also explores layer-wise training for FedSSL, in which the authors propose a depth dropout technique which aims to reduce both computation and communication overhead but may lead to a slight decrease in performance. In contrast to the above studies, our work offers an in-depth exploration of layer-wise training in the context of FedSSL. Moreover, as we have previously demonstrated, layer-wise training alone may not achieve the same level of performance as end-to-end training. To bridge this gap, we introduce LW-FedSSL, a layer-wise training approach that can compete end-to-end training with significantly lower client resource requirements. In addition, we explore a progressive training approach called Prog-FedSSL, which outperforms end-to-end training while requiring fewer resources.

#### IV. PROPOSED METHOD

##### A. LW-FedMoCo

Firstly, we discuss the pure layer-wise training baseline, referred to as LW-FedMoCo. Fig. 3 illustrates the local training process of LW-FedMoCo across different stages. For an encoder  $F$  with a total of  $S$  layers, the training process is divided into  $S$  stages. Each stage  $s \in [1, S]$  runs for a fixed number of FL communication rounds,  $R_s$ . The training process starts with an empty encoder  $F$  without any layers, and each stage  $s$  sequentially adds a new layer  $L_s$  to  $F$ , gradually increasing its depth. During stage  $s$ , only the corresponding layer  $L_s$

**Algorithm 2** LW-FedSSL (*Client-side*)

---

**Input:** encoder  $F$ , projection head  $H$ , prediction head  $P$ , local dataset  $D^i$ , number of local epochs  $E$ , momentum  $\mu$ , temperature  $\tau$ , weight term  $\alpha$   
**Output:** layer  $L_s^i$ , local projection head  $H^i$ , local prediction head  $P^i$

- 1: **Client executes:**
- 2:  $\text{Local\_SSL}(i, F, H, P)$ :
- 3: Online branch:  $F^i \leftarrow F$  and  $H^i \leftarrow H$  and  $P^i \leftarrow P$
- 4: Target branch:  $F_k^i \leftarrow F$  and  $H_k^i \leftarrow H$
- 5: **for** epoch  $e = 1, 2, \dots, E$  **do**
- 6:   **for** each batch  $x \in D^i$  **do**
- 7:      $x_1 \leftarrow \text{Augment}(x)$  and  $x_2 \leftarrow \text{Augment}(x)$
- 8:      $z_1 \leftarrow F(x_1)$  and  $z_2 \leftarrow F(x_2)$
- 9:      $z_1^i \leftarrow F^i(x_1)$  and  $z_2^i \leftarrow F^i(x_2)$
- 10:      $q_1^i \leftarrow P^i(H^i(z_1^i))$  and  $q_2^i \leftarrow P^i(H^i(z_2^i))$
- 11:      $k_1^i \leftarrow H_k^i(F_k^i(x_1))$  and  $k_2^i \leftarrow H_k^i(F_k^i(x_2))$
- 12:      $\ell_{\text{con}} \leftarrow \ell(q_1^i, k_2^i, \tau) + \ell(q_2^i, k_1^i, \tau)$       Eq. (2)
- 13:      $\ell_{\text{align}} \leftarrow \ell(z_1^i, z_2, \tau) + \ell(z_2^i, z_1, \tau)$       Eq. (3)
- 14:      $\mathcal{L} \leftarrow \ell_{\text{con}} + \alpha \ell_{\text{align}}$
- 15:      $F^i, H^i, P^i \leftarrow \text{Update}(\nabla \mathcal{L})$
- 16:      $F_k^i, H_k^i \leftarrow \text{Momentum\_Update}(F^i, H^i, \mu)$
- 17:  $L_s^i \leftarrow \text{Get active layer from } F^i$
- 18: **return**  $L_s^i, H^i, P^i$

---

is updated, while all prior layers  $L_1$  to  $L_{s-1}$  within  $F$  are frozen, serving only for inference. This strategy saves memory and computation, benefiting resource-constrained devices in FL environments. Moreover, in each communication round, clients are only required to send the active layer  $L_s$  (and the MLP heads) to the server for aggregation. Likewise, the server only needs to broadcast the aggregated layer  $L_s$  back to clients. This reduces both upload and download communication costs for clients. Although layer-wise training offers better resource efficiency than end-to-end training, there remains a notable performance gap in linear evaluation, as we have shown in Table I.

##### B. LW-FedSSL

To address the performance gap between layer-wise and end-to-end training for FedSSL, we propose LW-FedSSL by introducing two crucial mechanisms: *server-side calibration*, integrated at the server, and *representation alignment*, integrated into the local training process. Fig. 4 illustrates these two mechanisms of LW-FedSSL at stage  $s$ .

**Server-side calibration:** In layer-wise training, only the most recently added layer,  $L_s$ , is actively trained by clients at any given stage  $s$ . This may limit prior layers' ability to adapt to the newly added layer, potentially degrading the model's performance. Given a limited number of rounds  $R_s$  available for each stage, solely training  $L_s$  may prove insufficient to match the training received by the end-to-end strategy. On the other hand, increasing the number of rounds could introduce additional resource demands on clients. To tackle this, we can take advantage of resources available at the FL server. The

TABLE II: Given an encoder  $F$  with a total of  $S$  layers, we compare the characteristics of different approaches at stage  $s \in [1, S]$ .

	Training	Number of Stages	Initial Layers	New Layer	Frozen Layers	Active Layers	Server to Client (Download)	Client to Server (Upload)
<b>FedMoCo</b>	end-to-end	—	$L_1$ to $L_S$	—	—	$L_1$ to $L_S$	$L_1$ to $L_S$	$L_1$ to $L_S$
<b>LW-FedMoCo</b>	layer-wise	$S$	—	$L_s$	$L_1$ to $L_{s-1}$	$L_s$	$L_s$	$L_s$
<b>LW-FedSSL</b>	layer-wise	$S$	—	$L_s$	$L_1$ to $L_{s-1}$	$L_s$	$L_1$ to $L_s$	$L_s$
<b>Prog-FedSSL</b>	progressive	$S$	—	$L_s$	—	$L_1$ to $L_s$	$L_1$ to $L_s$	$L_1$ to $L_s$

server can contribute by training the current sub-model on a small auxiliary dataset,  $D^g$ , at the end of every communication round. Specifically, following the aggregation process, the server can train the aggregated encoder  $F$  across all existing layers (i.e.,  $L_1$  to  $L_s$ ) before broadcasting  $F$  back to the clients. The auxiliary dataset  $D^g$  may originate from a public dataset with a different data distribution than that of the clients' data, as the server cannot directly access data within clients. Furthermore,  $D^g$  may typically be unlabeled, requiring server-side training to also utilize an SSL approach. Training across all existing layers in the current sub-model plays a crucial role in calibrating the layers to function harmoniously. Also, our assumption regarding the auxiliary data at the server can be reasonably met, since in practice, the server may require a small dataset for various purposes, such as performance monitoring, pre-training, distillation, and other tasks in the FL context [23], [7], [24], [25], [26]. Particularly for FedSSL tasks, probing datasets may be necessary at the server to monitor and ensure smooth training progress.

**Representation alignment:** FL clients often exhibit distinct local data distributions resulting from diverse device usage patterns and application settings. Such data heterogeneity can introduce bias to the local training process, negatively affecting the performance of the global model. To mitigate this, some studies [27], [28] encourage local training processes across different clients to converge toward parameters that are closely aligned with the global parameters. Often, this is achieved by aligning the representations of local models with those of the global model while simultaneously pushing them away from old representations (from old local models of previous FL rounds) [27]. In contrast, our representation alignment mechanism does not require old local parameters. As a result, clients no longer need to store and perform inference on old parameters, reducing the overhead. Given a positive pair of views,  $x_q$  and  $x_{k+}$ , our approach uses local encoder  $F^i$  and the global encoder  $F$  to extract local representation  $z^i = F^i(x_q)$  and positive global representation  $z^+ = F(x_{k+})$ . Negative global representations  $z^-$  are extracted from other samples. Similar to Equation 2, we can calculate the alignment loss as

$$\ell(z^i, z, \tau) = -\log \frac{\exp(z^i \cdot z^+ / \tau)}{\exp(z^i \cdot z^+ / \tau) + \sum_{j=1}^K \exp(z^i \cdot z_j^- / \tau)}, \quad (3)$$

where  $z = (z^+, \{z_j^-\}_{j=1}^K)$ . This loss can be integrated into local training as an auxiliary loss for regularization, with a weight term  $\alpha$  to control its contribution.

The server-side calibration mechanism trains all existing layers in the global model to facilitate smooth collaboration

between them. However, during local training, updates only to the active layer may disrupt this cohesion. To mitigate this, representation alignment encourages the updates of the local model to remain closely aligned with the parameters of the global model. This prevents complete overwriting and helps preserve the layer cohesion established by server-side calibration, while also allowing local models to incorporate local information from their respective local datasets. Additionally, representation alignment prevents extensive divergence between different local models, enabling a more effective FL aggregation process. In Section V-C, we empirically show that server-side calibration and representation alignment mechanisms are complementary for improving the effectiveness of layer-wise training. Integrating these mechanisms enables LW-FedSSL to compete with end-to-end training, all the while substantially reducing resource demands on FL clients. The details of LW-FedSSL are presented in Algorithms 1 and 2. Algorithm 1 outlines the server-side execution, which handles gradual increase in the model depth based on stage, server-side calibration mechanism, and aggregation. Each client executes Algorithm 2, performing local SSL training with representation alignment for regularization.

### C. Prog-FedSSL

Inspired by ProgFed in [18], we also explore progressive training for FedSSL, denoted as Prog-FedSSL. Similar to layer-wise training, progressive training also starts with an empty encoder  $F$ , appending a new layer  $L_s$  to  $F$  at each stage  $s$ . However, in contrast to updating only a single layer  $L_s$ , progressive training updates all existing layers (i.e.,  $L_1$  to  $L_s$ ) during each stage  $s$ . This distinction results in higher computation and communication costs for Prog-FedSSL than layer-wise training approaches. Nonetheless, when compared with end-to-end training, which requires clients to train a full model with  $S$  layers (i.e.,  $L_1$  to  $L_S$ ) at each round, Prog-FedSSL enables clients to train only a sub-model with  $s$  layers ( $s \leq S$ ). Moreover, clients only need to exchange the sub-model with the server. In essence, Prog-FedSSL saves both computation and communication costs for  $(S - s)$  layers at each stage  $s$  compared to end-to-end training. As we will demonstrate in Section V-B, progressive training outperforms both layer-wise and end-to-end training approaches. Nevertheless, it is important to note that the memory requirement of progressive training gradually increases as the stages progress, becoming equivalent to that of end-to-end training at the final stage (i.e., when  $s = S$ ). This may limit low-memory devices from participating in the FL process, whereas the memory requirement of layer-wise training is significantly

TABLE III: Linear evaluation and fine-tuning performance of different approaches. We conduct the experiments three times with different seeds. We compare the memory, FLOPs, and communication costs (download + upload) for a local training process. FedMoCo, FedBYOL, and FedSimCLR correspond to MoCo v3 [11], BYOL [29], and SimCLR [1] integrated with FL. For FedSimCLR, we use a batch size of 512. Three best values, except for the centralized MoCo v3, are marked in **bold**.

	Cost			Linear Evaluation				Fine-tune			
	Memory	FLOPs	Comm.	CIFAR-10	CIFAR-100	STL-10	Tiny ImageNet	CIFAR-10	CIFAR-100	STL-10	Tiny ImageNet
<b>MoCo v3</b>	–	–	–	$70.82 \pm 0.06$	$46.09 \pm 0.45$	$63.84 \pm 0.42$	$28.61 \pm 0.45$	$86.27 \pm 0.26$	$64.57 \pm 0.38$	$69.78 \pm 0.91$	$43.95 \pm 0.48$
<b>Scratch</b>	–	–	–	$23.47 \pm 1.20$	$5.83 \pm 0.42$	$17.50 \pm 1.00$	$2.68 \pm 1.09$	$63.23 \pm 0.94$	$41.69 \pm 0.58$	$44.08 \pm 0.13$	$27.99 \pm 0.33$
<b>FedMoCo</b>	$1.00 \times$	$1.00 \times$	$1.00 \times$	$60.64 \pm 0.14$	<b><math>34.66 \pm 0.42</math></b>	$54.96 \pm 0.03$	<b><math>20.55 \pm 0.28</math></b>	$79.46 \pm 0.32$	$58.70 \pm 0.32$	$62.59 \pm 0.36$	<b><math>40.62 \pm 0.28</math></b>
<b>FedBYOL</b>	$1.00 \times$	$1.00 \times$	$1.00 \times$	$55.38 \pm 0.03$	$28.64 \pm 0.04$	$51.01 \pm 0.07$	$16.34 \pm 0.05$	$77.25 \pm 0.11$	$56.92 \pm 0.39$	$60.36 \pm 0.18$	$39.58 \pm 0.39$
<b>FedSimCLR</b>	$0.99 \times$	$1.49 \times$	$1.00 \times$	<b><math>62.59 \pm 0.03</math></b>	<b><math>36.94 \pm 0.08</math></b>	<b><math>57.89 \pm 0.06</math></b>	<b><math>21.81 \pm 0.07</math></b>	$79.50 \pm 0.39$	$58.45 \pm 0.15$	<b><math>63.15 \pm 0.24</math></b>	<b><math>41.43 \pm 0.27</math></b>
<b>LW-FedMoCo</b>	$0.25 \times$	<b><math>0.35 \times</math></b>	<b><math>0.08 \times</math></b>	$50.39 \pm 0.26$	$27.32 \pm 0.14$	$47.62 \pm 0.29$	$15.11 \pm 0.41$	<b><math>84.03 \pm 0.18</math></b>	<b><math>61.02 \pm 0.26</math></b>	$59.56 \pm 0.40$	$39.85 \pm 0.25$
<b>LW-FedSSL</b>	<b><math>0.30 \times</math></b>	<b><math>0.48 \times</math></b>	<b><math>0.31 \times</math></b>	<b><math>61.83 \pm 0.42</math></b>	$32.11 \pm 0.30$	<b><math>55.56 \pm 0.61</math></b>	$17.26 \pm 0.24$	<b><math>84.63 \pm 0.25</math></b>	<b><math>61.18 \pm 0.21</math></b>	<b><math>66.95 \pm 0.24</math></b>	$39.83 \pm 0.23$
<b>Prog-FedSSL</b>	$1.00 \times$	$0.57 \times$	$0.54 \times$	$65.76 \pm 0.10$	<b><math>39.45 \pm 0.06</math></b>	<b><math>60.83 \pm 0.07</math></b>	<b><math>23.02 \pm 0.51</math></b>	<b><math>86.21 \pm 0.23</math></b>	<b><math>64.01 \pm 0.41</math></b>	<b><math>69.45 \pm 0.54</math></b>	<b><math>41.04 \pm 0.13</math></b>

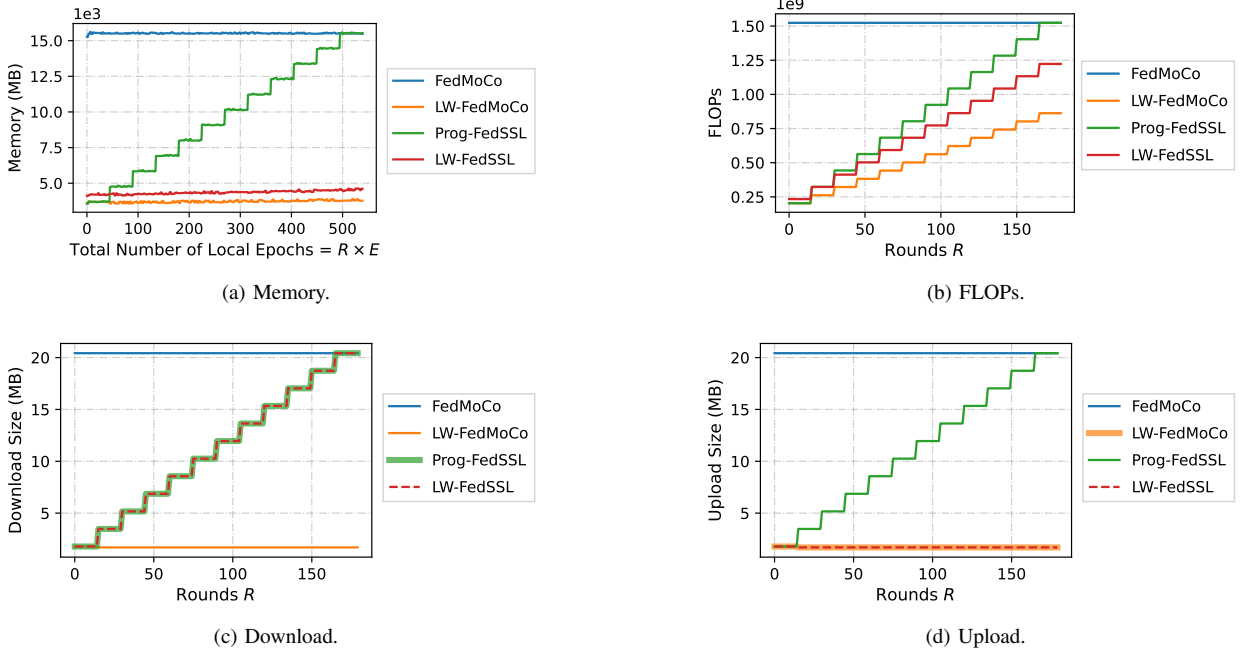


Fig. 5: Computation and communication resources required for a local training process. (a) Memory requirement. (b) FLOPs consumption. (c) Download size. (d) Upload size.

lower due to training a single layer  $L_s$  at a time. We compare the different characteristics of FedMoCo (end-to-end), LW-FedMoCo, LW-FedSSL, and Prog-FedSSL in Table II. Fig. 15 in Appendix A illustrates FedMoCo, LW-FedMoCo, and Prog-FedSSL at stage  $s$ .

## V. EXPERIMENT

### A. Experimental setup

Unless otherwise stated, we use the following settings in our experiments. We use a ViT-Tiny [30] backbone with 12 transformer blocks (i.e.,  $S = 12$ ) as encoder  $F$ . We use an input dimension of  $32 \times 32 \times 3$  with a patch size of 4. The projection head  $H$  and the prediction head  $P$  are implemented as a 3-layer MLP and a 2-layer MLP, respectively. For both  $H$  and  $P$ , the hidden layer dimensions are set to 4096 and the output dimension is set to 256. We follow MoCo v3 [11] for SSL, except that we train the patch projection layer. The total number of communication rounds  $R$  is set to 180 and is evenly

distributed across different stages  $s \in [1, S]$ . This results in 15 rounds per stage (i.e.,  $R_s = R/S = 15$ ). We use 10 FL clients, where each performs local training for 3 epochs using the AdamW optimizer with a base learning rate of  $1.5e-4$  and a weight decay of  $1e-5$ . We linearly scale the learning rate as  $base\ learning\ rate \times batch\ size/256$  [31], [32] and use a cosine decay schedule during training. The batch size is set to 1024. We set the momentum  $\mu$  to 0.99 and the temperature  $\tau$  to 0.2. Data augmentations for view creation include random resized crop, color jitter, grayscale, horizontal flip, Gaussian blur, and solarization. For the server-side calibration mechanism, we use the same settings as in local training. We transfer the layer weights from  $L_{s-1}$  to  $L_s$  at the beginning of each stage  $s$  since we observe a slight performance improvement for the baseline LW-FedMoCo with weight transfer. Therefore, to ensure fairness, we also incorporate weight transfer in LW-FedSSL and Prog-FedSSL. We uniformly split the unlabeled data portion of STL-10 dataset [33] to construct the local data of FL clients.

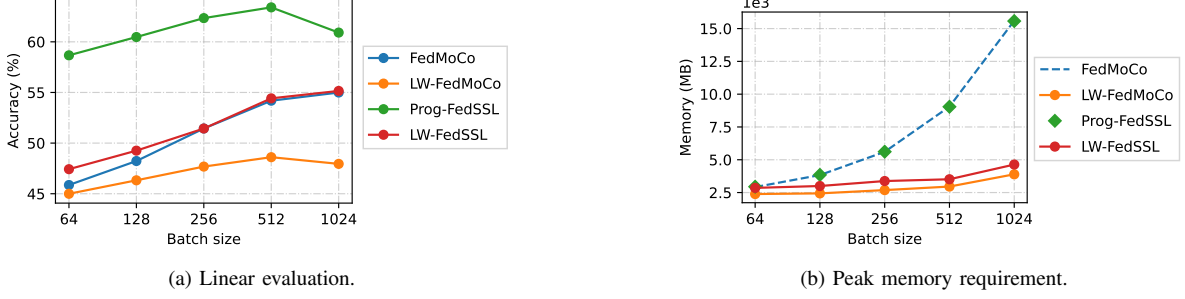


Fig. 6: Impact of batch size on different approaches. (a) Linear evaluation results on the STL-10 dataset and (b) peak memory requirements for different batch sizes.

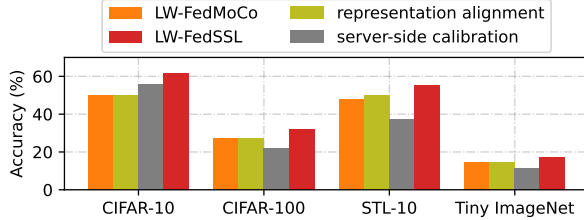


Fig. 7: Linear evaluation performance of LW-FedSSL, the baseline LW-FedMoCo, and its two variants incorporating either server-side calibration or representation alignment. Weight transfer between blocks is not performed for these two variants, as they demonstrate better performance without it.

To evaluate the performance, we use the CIFAR-10/100 [34], STL-10 (labeled portion), and Tiny ImageNet [35] datasets. For LW-FedSSL, we use only 10% of CIFAR-10 training data, excluding labels, as auxiliary data  $D^g$ . For the representation alignment mechanism, we set  $\alpha$  to 0.01.

Following common practices, we primarily use linear evaluation for performance comparison [36], [37], [1]. The projection head  $H$  and prediction head  $P$  are discarded, and a linear classifier is trained on top of the frozen encoder  $F$  for 20 epochs using a batch size of 256. We use the AdamW optimizer with a base learning rate of 3e-2 and a weight decay of 1e-5. The learning rate decays with a cosine schedule. We use the RandAugment function available in the PyTorch [38] framework for augmentation. For fine-tuning, we set the base learning rate to 1e-3 and the number of epochs to 40 with a warmup period of 10 epochs. Other settings are similar to those of linear evaluation.

### B. Performance and Resource Comparison

Table III compares the performance of different approaches. In terms of linear evaluation, LW-FedSSL demonstrates comparable performance to the end-to-end training of FedMoCo and significantly outperforms the purely layer-wise training of LW-FedMoCo. LW-FedSSL also outperforms or holds a competitive position against FedMoCo in fine-tuning. The progressive training approach, Prog-FedSSL, outperforms all other approaches in both linear evaluation and fine-tuning performance. Interestingly, the fine-tuning performance of

FedMoCo is even lower than that of LW-FedMoCo in some cases. Please note that we apply the same fine-tuning settings, which may not be optimal for all approaches.

In Fig. 5, we present resource requirements for a single client. Fig. 5a measures the memory usage at each local epoch, showing that the memory requirement of LW-FedSSL is 3.3 $\times$  lower than that of FedMoCo at peak usage. The memory usage of Prog-FedSSL gradually increases and eventually matches that of FedMoCo in the final stage. Fig. 5b shows that LW-FedSSL also maintains a lower FLOPs requirement than FedMoCo, with 2.1 $\times$  lower total FLOPs consumption. Additional memory and FLOPs requirements of LW-FedSSL over LW-FedMoCo arise from the representation alignment mechanism, which requires inference on the global model to obtain global representations.

In Figures 5c and 5d, we investigate the communication cost required for model exchange (download and upload) between the server and a client. Note that we only consider the encoder part for comparison, excluding the projection and prediction heads, which are common to all approaches with constant communication costs. In FedMoCo, a client needs to exchange the full encoder with the server at each communication round. Meanwhile, in LW-FedMoCo, a client only needs to exchange the active layer (i.e.,  $L_s$ ). Thus, both FedMoCo and LW-FedMoCo result in constant download and upload costs across different communication rounds. For Prog-FedSSL, both download and upload costs gradually increase as the number of active layers (i.e.,  $L_1$  to  $L_s$ ) grows with the stage  $s$ . As for LW-FedSSL, a client needs to download layers  $L_1$  to  $L_s$  from the server, as these are updated through the server-side calibration mechanism. However, the client uploads a single layer  $L_s$ , as only it is updated by the local training process. Therefore, the download cost of LW-FedSSL increases with each step  $s$ , while the upload cost remains constant. Upon comparing the total communication cost over 180 rounds, LW-FedSSL is 1.8 $\times$  cheaper in terms of download cost and 12 $\times$  cheaper in terms of upload cost compared to FedMoCo.

### C. Ablation Study

In Fig. 7, we compare LW-FedSSL with the baseline LW-FedMoCo and its two variants, which solely incorporate either server-side calibration or representation alignment. Incorporating server-side calibration improves performance

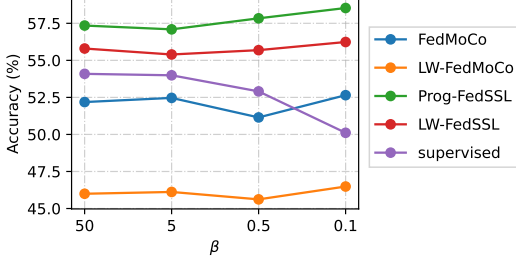


Fig. 8: Different levels of data heterogeneity. Linear evaluation results are shown for the STL-10 dataset.

TABLE IV: Linear evaluation results of LW-FedSSL with different amounts of auxiliary data.

Ratio	CIFAR-10	CIFAR-100	STL-10	Tiny ImageNet
10% ( $D^g$ only)	43.75	20.03	40.97	9.77
1%	47.80	23.69	43.65	12.76
10%	61.83	32.25	55.15	17.26
100%	<b>79.63</b>	<b>47.09</b>	<b>69.52</b>	<b>26.75</b>

on the CIFAR-10 dataset (from which the auxiliary data is sampled), but leads to a decline on other datasets. This decline may result from conflicting update directions between training on auxiliary data and the local training. Compared to the baseline, incorporating representation alignment obtains better performance on the STL-10 dataset, with comparable performance on the others. Meanwhile, LW-FedSSL, which incorporates both mechanisms, consistently outperforms the baseline across all datasets. The server-side calibration mechanism facilitates smooth collaboration between different layers of the model. Meanwhile, representation alignment encourages the weights of the local model to remain closely aligned with those of the global model. This helps maintain layer cohesion established by the server-side calibration mechanism during the local training process. Fig. 7 suggests that instead of acting independently, server-side calibration and representation alignment are complementary for improving the performance of layer-wise training.

#### D. Amount of Auxiliary Data

The server-side calibration mechanism of LW-FedSSL relies on the auxiliary dataset  $D^g$ . We vary the amount of auxiliary data at the server by sampling 1%, 10%, and 100% of the CIFAR-10 training data. We also conduct a centralized end-to-end SSL training using only the auxiliary data at the sever. The results in Table IV indicate that the performance of LW-FedSSL improves with an increase in the amount of data.

#### E. Batch Size

SSL approaches tend to perform better with larger batch sizes due to a greater number of negative samples [1]. To investigate this, we set the local training batch size to 64, 128, 256, 512, and 1024. Fig. 6a indicates that layer-wise training approaches, LW-FedMoCo and LW-FedSSL, also tend

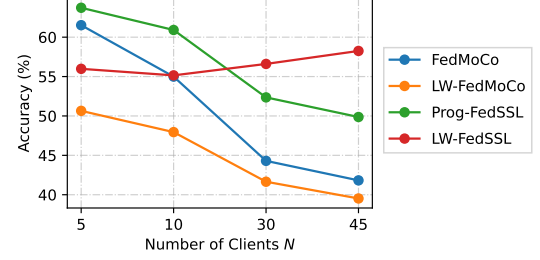


Fig. 9: Total number of clients. Linear evaluation results are shown for the STL-10 dataset.

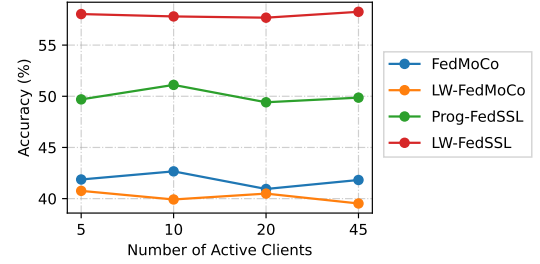


Fig. 10: Number of participating clients in each FL round. The total number of clients is set to 45. Linear evaluation results are shown for the STL-10 dataset.

to improve with increased batch size, similar to end-to-end SSL training. Fig. 6b reports peak memory requirements for each setting. Given that Prog-FedSSL does not freeze the layers, its peak memory requirement (at the last stage) is equivalent to that of FedMoCo. Memory requirements for FedMoCo and Prog-FedSSL sharply rise as the batch size grows, while those of LW-FedMoCo and LW-FedSSL remain relatively flat.

#### F. Data Heterogeneity

Data heterogeneity is one of the main challenges in an FL environment. In this experiment, we use the Tiny ImageNet dataset to construct the local data of clients. We control the data heterogeneity based on data labels and the Dirichlet distribution [39]. The concentration parameter  $\beta$  in the Dirichlet distribution determines the strength of data heterogeneity, with a lower  $\beta$  value indicating a higher degree of heterogeneity. The labels are used here to set up the clients' data partitions and are not used during training (except for the supervised baseline). Fig. 8 presents the linear evaluation results for different  $\beta$  values. For the supervised baseline, an end-to-end classification model is trained with vanilla FL using labeled data, and then only the encoder part is kept for linear evaluation. Notably, performance of the supervised approach diminishes as the degree of data heterogeneity increases. In contrast, other approaches employing SSL are relatively more robust to different  $\beta$  values. This observation conforms with prior studies [8] that highlight the robustness of SSL to data heterogeneity in FL environments. Fig. 8 indicates that layer-wise training also exhibits robustness to data heterogeneity inherent in end-to-end SSL training.

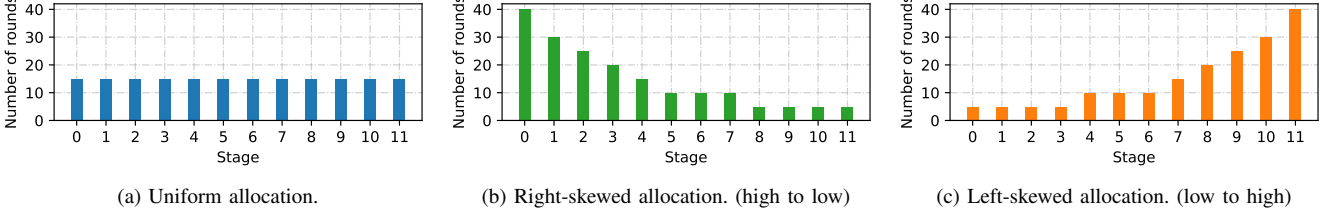


Fig. 11: Number of rounds per stage.

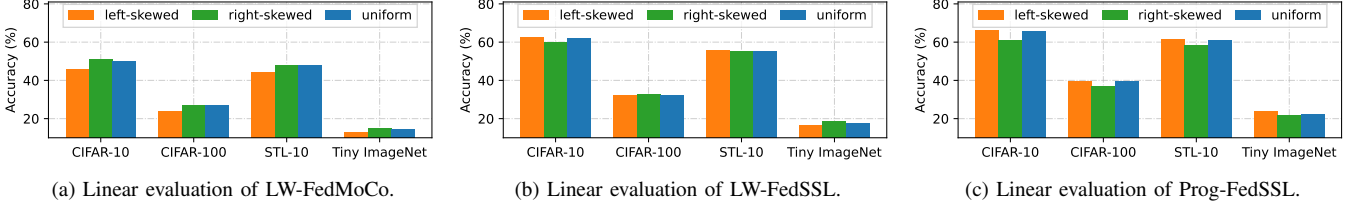


Fig. 12: Impact of number of rounds per stage.

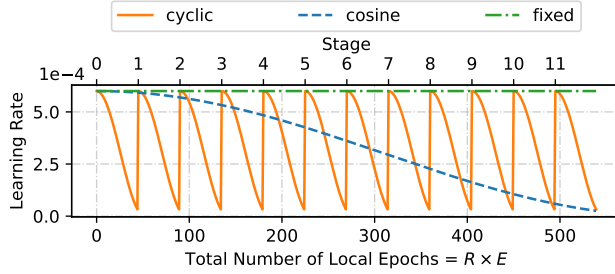


Fig. 13: Learning rate strategies.

#### G. Total Number of Clients

To investigate the impact of the number of clients  $N$ , we conduct experiments with  $N$  set to 5, 10, 30, and 45. For each setting, we uniformly partition the unlabeled data portion of the STL-10 dataset into  $N$  local datasets. Therefore, the total number of data samples remains constant across all settings. Linear evaluation results with varying  $N$  values are shown in Fig. 9. We can observe that all approaches, except LW-FedSSL, experience a drop in performance as the number of clients increases. Integration of representation alignment mechanism enables LW-FedSSL to maintain good performance even in scenarios with a large number of clients [27].

#### H. Number of Participating Clients

In FL environments, it is common for only a subset of clients to participate in training at any given time. Therefore, we experiment with the number of clients active for training at each FL round. We set the total number of clients to 45 and randomly sample 5, 10, 20, and 45 clients at each FL round. The linear evaluation results in Fig. 10 demonstrate that LW-FedSSL can maintain its performance even with a small proportion of participating clients in each FL round.

#### I. Distribution of Number of Rounds Per Stage

In our experiments, the number of rounds for each layer-wise training stage is uniformly distributed. As shown in Fig. 11, we explore two alternative settings: one where a larger number of rounds is allocated to earlier stages, and the other where a larger number of rounds is allocated to later stages. We refer to these settings as “right-skewed allocation” and “left-skewed allocation”, respectively. The total number of rounds across all settings remains constant at 180. The results are shown in Fig. 12.

For LW-FedMoCo, the left-skewed setting results in the worst performance. In this setting, earlier layers receive updates for a small number of rounds, potentially lowering the quality of their output features. Even though later layers are trained for a large number of rounds, poor output features from the early layers may degrade the output of subsequent layers. The other two settings achieve comparable performance. As for LW-FedSSL, it allows early layers to continuously receive updates through the server-side calibration mechanism, which improves the performance of the left-skewed setting in most cases.

In the case of Prog-FedSSL, none of the layers from prior stages are frozen, allowing a layer  $L_s$  to receive training for all the rounds allocated through stages  $s$  to  $S$ . This means that in a left-skewed allocation scenario, if we assign 10 rounds to stage  $S-1$  and 50 rounds to stage  $S$ , then the layer  $L_{S-1}$  undergoes training for a total of 60 rounds (since it is not frozen), while  $L_S$  is trained for 50 rounds. However, if we reverse the scenario in the right-skewed allocation, i.e., assign 50 rounds to stage  $S-1$  and 10 rounds to stage  $S$ , the layer  $L_{S-1}$  still undergoes training for 60 rounds, while  $L_S$  is trained only for 10 rounds. As a result, the left-skewed setting achieves better performance than the right-skewed setting; however, it would also consume more computation resources. The same case also applies to the server-side calibration mechanism of LW-FedSSL.

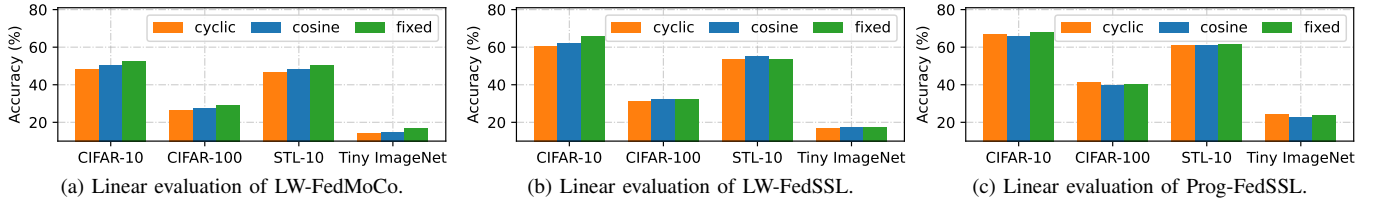


Fig. 14: Impact of different learning rate strategies.

#### *J. Learning Rate Strategy*

By default, we use cosine decay scheduling for the learning rate. We explore different learning rate strategies for LW-FedMoCo, LW-FedSSL, and Prog-FedSSL, including a fixed learning rate and cosine decay scheduling for each training stage, which we refer to as “*cyclic*”. Fig. 13 illustrates how the learning rate changes at each local epoch for different strategies, and the results are presented in Fig. 14. For LW-FedMoCo, using a fixed learning rate achieves the best performance, and also for both LW-FedSSL and Prog-FedSSL, simply using a fixed learning rate can be a decent choice. A fixed learning rate may allow layers in later stages to receive effective updates, whereas in cosine decay scheduling, later layers undergo minimal updates due to a small learning rate. While the cyclic learning rate pattern proves to work decently for Prog-FedSSL, it may not be suitable for LW-FedMoCo and LW-FedSSL. As seen in Fig. 13, the learning rate for cyclic strategy drops quickly in each stage when only a limited number of rounds are available. This can impact layer-wise training, where a layer receives training only in its corresponding stage. (For LW-FedSSL with a fixed learning rate, we do not use weight transfer, as it demonstrates improved performance.)

## VI. CONCLUSION

Edge devices in distributed environments often struggle to meet the computation and communication requirements of FedSSL. In response to these challenges, we propose a layer-wise training approach called LW-FedSSL, enabling FL clients to reduce their resource requirements. Our experiments demonstrate that LW-FedSSL has a  $3.3 \times$  lower memory requirement,  $2.1 \times$  lower total FLOPs consumption, and  $3.2 \times$  cheaper total transmission cost (download + upload), while achieving comparable performance to its end-to-end training counterpart. Furthermore, we explore a progressive training approach called Prog-FedSSL, which remains more resource-efficient than end-to-end training, with significantly improved performance.

## APPENDIX A

### ADDITIONAL DETAILS

## A. Self-supervised Learning

Algorithm 3 describes the detailed training procedure of MoCo v3 [11].

TABLE V: Linear evaluation results of LW-FedSSL with different  $\alpha$  values.

$\alpha$	CIFAR-10	CIFAR-100	STL-10	Tiny ImageNet
<b>0.01</b>	<b>61.83</b>	<b>32.25</b>	<b>55.15</b>	<b>17.26</b>
<b>0.1</b>	59.21	30.53	52.25	16.14
<b>1</b>	56.92	27.13	52.34	13.00
<b>10</b>	55.84	24.00	50.67	11.66

TABLE VI: Linear evaluation results with and without weight transfer (WT).

	WT	CIFAR-10	CIFAR-100	STL-10	Tiny ImageNet
LW-FedMoCo	w/o	49.38	25.15	46.41	14.35
	w/	<b>50.09</b>	<b>27.16</b>	<b>47.95</b>	<b>14.64</b>
LW-FedSSL	w/o	<b>63.27</b>	31.84	53.30	<b>18.37</b>
	w/	61.83	<b>32.25</b>	<b>55.15</b>	17.26
Prog-FedSSL	w/o	65.07	<b>39.53</b>	58.79	<b>23.74</b>
	w/	<b>65.64</b>	39.52	<b>60.91</b>	22.43

### B. Data Distribution

Fig. 16 illustrates the data distribution among clients for different  $\beta$  values used in Section V-F. Lower  $\beta$  values correspond to increasingly heterogeneous data distributions among clients.

### C. Details on FLOPs Calculation

Here, we discuss the details on FLOPs calculation used in Section V-B. In layer-wise training, calculating FLOPs for inactive (frozen) layers involves simply considering FLOPs

---

**Algorithm 3** Self-supervised learning (SSL)

**Input:** encoder  $F$ , projection head  $H$ , prediction head  $P$ , dataset  $D$ , number of epochs  $E$ , momentum  $\mu$ , temperature  $\tau$   
**Output:** encoder  $F$ , projection head  $H$ , prediction head  $P$

```

1: target branch:  $F_k \leftarrow F$  and  $H_k \leftarrow H$ 
2: for epoch  $e = 1, 2, \dots, E$  do
3:   for each batch  $x \in D$  do
4:      $x_1 \leftarrow \text{Augment}(x)$  and  $x_2 \leftarrow \text{Augment}(x)$ 
5:      $q_1 \leftarrow P(H(F(x_1)))$  and  $q_2 \leftarrow P(H(F(x_2)))$ 
6:      $k_1 \leftarrow H_k(F_k(x_1))$  and  $k_2 \leftarrow H_k(F_k(x_2))$ 
7:      $\ell_{\text{con}} \leftarrow \ell(q_1, k_2, \tau) + \ell(q_2, k_1, \tau)$  Eq. (2)
8:      $F, H, P \leftarrow \text{Update}(\nabla \ell_{\text{con}})$ 
9:      $F_k, H_k \leftarrow \text{Momentum\_Update}(F, H, \mu)$ 
10: return  $F, H, P$ 

```

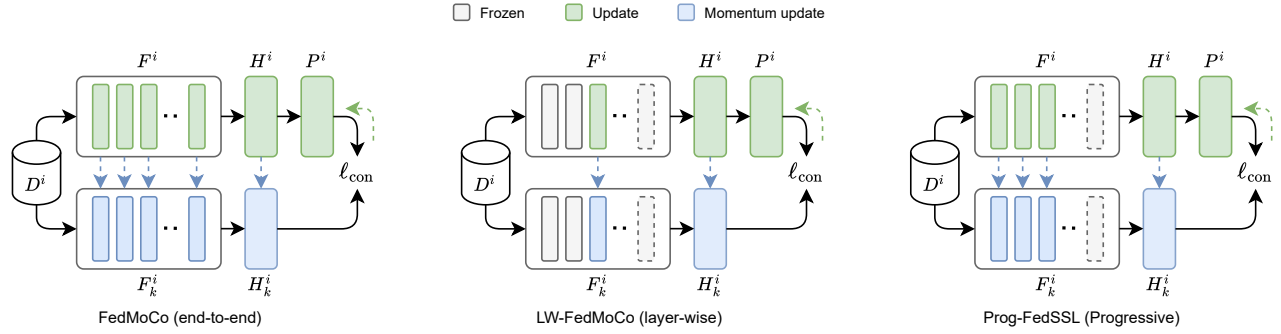


Fig. 15: Comparison between FedMoCo (left), LW-FedMoCo (center), and Prog-FedSSL (right) at stage  $s$ .

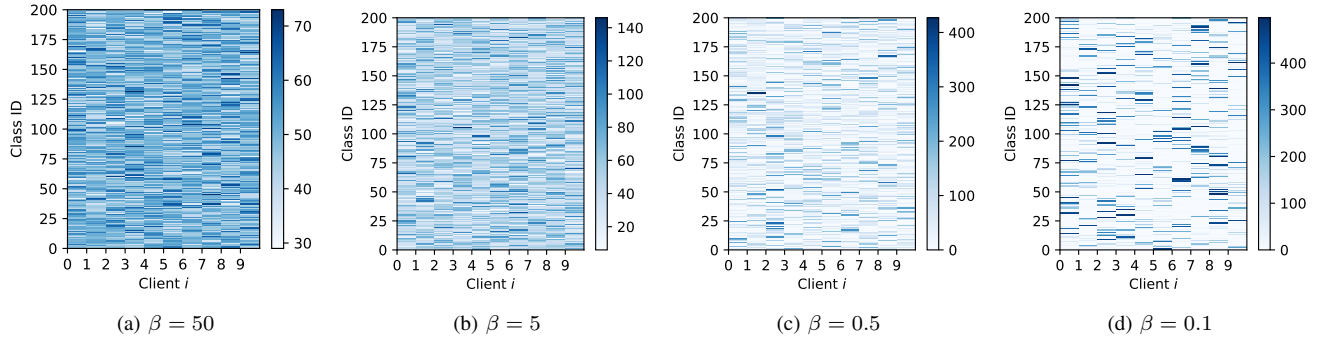


Fig. 16: Client data distribution with different  $\beta$  values for the Tiny ImageNet dataset. A darker color denotes a higher number of data samples for a specific class in a client.

TABLE VII: Projection head  $H$ .

Layer	Input dimension	Output dimension	Batch norm	ReLU
1	192	4096	✓	✓
2	4096	4096	✓	✓
3	4096	256	✓	✗

associated with the forward pass. However, for active layers, the calculation must account for both the forward and backward passes. While numerous works have addressed FLOPs calculation for the forward pass (inference), limited studies are available on the practice of FLOPs calculation for the backward pass. Notably, existing works related to layer-wise training [18], [19] also do not provide specific details on how FLOPs are computed. Some studies [40], [41], [42], [43] suggest that the number of operations in a backward pass of a neural network is often twice that of a forward pass. Following these studies, we adopt a backward-forward ratio of 2:1 to calculate the total FLOPs for active layers. We use the FlopCountAnalysis tool in the fvcore [44] library for calculating the FLOPs of the forward pass. We only consider a single input sample for FLOPs calculation.

## APPENDIX B ADDITIONAL EXPERIMENTS

### A. Weight of Representation Alignment

In LW-FedSSL, the weight term  $\alpha$  controls the regularization strength of the representation alignment mechanism in

TABLE VIII: Prediction head  $P$ .

Layer	Input dimension	Output dimension	Batch norm	ReLU
1	256	4096	✓	✓
2	4096	256	✓	✗

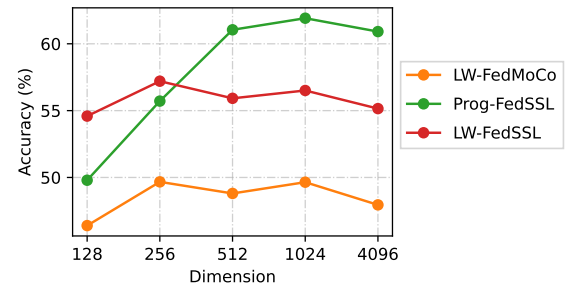


Fig. 17: Hidden layer dimension in the MLP heads. Linear evaluation results are shown for the STL-10 dataset.

the local training process. We explore different  $\alpha$  values in Table V. Based on the results, we set the default value of  $\alpha$  to 0.01.

### B. Weight Transfer

For LW-FedMoCo, LW-FedSSL, and Prog-FedSSL, we transfer the weights of the prior layer,  $L_{s-1}$ , to the subsequent layer,  $L_s$ , at the beginning of a new stage  $s$ . Here, we investigate the impact of weight transfer on the performance of

these approaches. Table VI demonstrates that weight transfer can improve the linear evaluation performance of the baseline LW-FedMoCo across different downstream datasets. For LW-FedSSL, weight transfer improves the performance on STL-10 and CIFAR-100 but decreases on CIFAR-10 and Tiny ImageNet datasets. Similarly, in the case of Prog-FedSSL, weight transfer leads to improved performance on STL-10 but a slight decrease on Tiny ImageNet, while maintaining comparable performance on other datasets. Notably, weight transfer consistently improves performance across all approaches on the STL-10 dataset, a case where the downstream data originates from a similar distribution as the unlabeled pre-training data within clients. This highlights a potential utility of weight transfer in the context of layer-wise training, where downstream data and pre-training data originate from a similar distribution (e.g., semi-supervised scenarios where only a portion of the data is labeled).

### C. Hidden Layer Dimension in MLP Heads

Following [11], we set the dimension of hidden layers in the projection head  $H$  and the prediction head  $P$  to 4096 by default. Tables VII and VIII describe the detailed structures of  $H$  and  $P$ , respectively. We further explore various dimensions, specifically 128, 256, 512, and 1024. The results in Fig. 17 indicate that Prog-FedSSL is relatively sensitive to the hidden layer dimension of the MLP heads.

## REFERENCES

- [1] T. Chen, S. Kornblith, M. Norouzi, and G. Hinton, “A simple framework for contrastive learning of visual representations,” in *International conference on machine learning*. PMLR, 2020, pp. 1597–1607.
- [2] K. He, H. Fan, Y. Wu, S. Xie, and R. Girshick, “Momentum contrast for unsupervised visual representation learning,” in *Proceedings of the IEEE/CVF conference on computer vision and pattern recognition*, 2020, pp. 9729–9738.
- [3] X. Chen and K. He, “Exploring simple siamese representation learning,” in *Proceedings of the IEEE/CVF conference on computer vision and pattern recognition*, 2021, pp. 15 750–15 758.
- [4] J. Konečny, H. B. McMahan, D. Ramage, and P. Richtárik, “Federated optimization: Distributed machine learning for on-device intelligence,” *arXiv preprint arXiv:1610.02527*, 2016.
- [5] B. McMahan, E. Moore, D. Ramage, S. Hampson, and B. A. y Arcas, “Communication-efficient learning of deep networks from decentralized data,” in *Artificial intelligence and statistics*. PMLR, 2017, pp. 1273–1282.
- [6] W. Zhuang, X. Gan, Y. Wen, S. Zhang, and S. Yi, “Collaborative unsupervised visual representation learning from decentralized data,” in *Proceedings of the IEEE/CVF international conference on computer vision*, 2021, pp. 4912–4921.
- [7] J. Li, L. Lyu, D. Iso, C. Chakrabarti, and M. Spranger, “Mocosfl: Enabling cross-client collaborative self-supervised learning,” in *The Eleventh International Conference on Learning Representations*, 2023. [Online]. Available: <https://openreview.net/forum?id=2QGJXyMNoPz>
- [8] L. Wang, K. Zhang, Y. Li, Y. Tian, and R. Tedrake, “Does learning from decentralized non-IID unlabeled data benefit from self supervision?” in *The Eleventh International Conference on Learning Representations*, 2023. [Online]. Available: <https://openreview.net/forum?id=2L9gzS80tA4>
- [9] A. Vaswani, N. Shazeer, N. Parmar, J. Uszkoreit, L. Jones, A. N. Gomez, Ł. Kaiser, and I. Polosukhin, “Attention is all you need,” *Advances in neural information processing systems*, vol. 30, 2017.
- [10] A. Dosovitskiy, L. Beyer, A. Kolesnikov, D. Weissenborn, X. Zhai, T. Unterthiner, M. Dehghani, M. Minderer, G. Heigold, S. Gelly, J. Uszkoreit, and N. Houlsby, “An image is worth 16x16 words: Transformers for image recognition at scale,” in *International Conference on Learning Representations*, 2021. [Online]. Available: <https://openreview.net/forum?id=YicbFdNTTy>
- [11] X. Chen, S. Xie, and K. He, “An empirical study of training self-supervised vision transformers,” in *2021 IEEE/CVF International Conference on Computer Vision (ICCV)*. Los Alamitos, CA, USA: IEEE Computer Society, oct 2021, pp. 9620–9629. [Online]. Available: <https://doi.ieeecomputersociety.org/10.1109/ICCV48922.2021.00950>
- [12] A. Van den Oord, Y. Li, and O. Vinyals, “Representation learning with contrastive predictive coding,” *arXiv e-prints*, pp. arXiv–1807, 2018.
- [13] W. Zhuang, Y. Wen, and S. Zhang, “Divergence-aware federated self-supervised learning,” *arXiv preprint arXiv:2204.04385*, 2022.
- [14] A. Saeed, F. D. Salim, T. Ozcelebi, and J. Lukkien, “Federated self-supervised learning of multisensor representations for embedded intelligence,” *IEEE Internet of Things Journal*, vol. 8, no. 2, pp. 1030–1040, 2020.
- [15] S. Ek, R. Rombourg, F. Portet, and P. Lalanda, “Federated self-supervised learning in heterogeneous settings: Limits of a baseline approach on har,” in *2022 IEEE International Conference on Pervasive Computing and Communications Workshops and other Affiliated Events (PerCom Workshops)*. IEEE, 2022, pp. 557–562.
- [16] G. E. Hinton, S. Osindero, and Y.-W. Teh, “A fast learning algorithm for deep belief nets,” *Neural Comput.*, vol. 18, no. 7, p. 1527–1554, jul 2006. [Online]. Available: <https://doi.org/10.1162/neco.2006.18.7.1527>
- [17] Y. Bengio, P. Lamblin, D. Popovici, and H. Larochelle, “Greedy layer-wise training of deep networks,” in *Proceedings of the 19th International Conference on Neural Information Processing Systems*, ser. NIPS’06. Cambridge, MA, USA: MIT Press, 2006, p. 153–160.
- [18] H.-P. Wang, S. Stich, Y. He, and M. Fritz, “Progfd: Effective, communication, and computation efficient federated learning by progressive training,” in *International Conference on Machine Learning*. PMLR, 2022, pp. 23 034–23 054.
- [19] P. Guo, W. Morningstar, R. Vemulapalli, K. Singhal, V. Patel, and P. Mansfield, “Towards federated learning under resource constraints via layer-wise training and depth dropout,” in *The 4th Workshop on practical ML for Developing Countries: learning under limited/low resource settings @ ICLR 2023*, 2023. [Online]. Available: [https://pml4dc.github.io/iclr2023/pdf/PML4DC\\_ICLR2023\\_5.pdf](https://pml4dc.github.io/iclr2023/pdf/PML4DC_ICLR2023_5.pdf)
- [20] S. Caldas, J. Konečny, H. B. McMahan, and A. Talwalkar, “Expanding the reach of federated learning by reducing client resource requirements,” *arXiv preprint arXiv:1812.07210*, 2018.
- [21] S. Horvath, S. Laskaridis, M. Almeida, I. Leontiadis, S. Venieris, and N. Lane, “Fjord: Fair and accurate federated learning under heterogeneous targets with ordered dropout,” *Advances in Neural Information Processing Systems*, vol. 34, pp. 12 876–12 889, 2021.
- [22] Z. Huo, D. Hwang, K. C. Sim, S. Garg, A. Misra, N. Siddhartha, T. Strohman, and F. Beaufays, “Incremental layer-wise self-supervised learning for efficient speech domain adaptation on device,” *arXiv preprint arXiv:2110.00155*, 2021.
- [23] F. Sattler, T. Korjakow, R. Rischke, and W. Samek, “Fedaux: Leveraging unlabeled auxiliary data in federated learning,” *IEEE Transactions on Neural Networks and Learning Systems*, 2021.
- [24] Y. L. Tun, M. N. Nguyen, C. M. Thwal, J. Choi, and C. S. Hong, “Contrastive encoder pre-training-based clustered federated learning for heterogeneous data,” *Neural Networks*, vol. 165, pp. 689–704, 2023. [Online]. Available: <https://www.sciencedirect.com/science/article/pii/S08936082023003192>
- [25] W. Zhang, X. Wang, P. Zhou, W. Wu, and X. Zhang, “Client selection for federated learning with non-iid data in mobile edge computing,” *IEEE Access*, vol. 9, pp. 24 462–24 474, 2021.
- [26] M. Yang, X. Wang, H. Zhu, H. Wang, and H. Qian, “Federated learning with class imbalance reduction,” in *2021 29th European Signal Processing Conference (EUSIPCO)*. IEEE, 2021, pp. 2174–2178.
- [27] Q. Li, B. He, and D. Song, “Model-contrastive federated learning,” in *Proceedings of the IEEE/CVF Conference on Computer Vision and Pattern Recognition (CVPR)*, June 2021, pp. 10 713–10 722.
- [28] T. Li, A. K. Sahu, M. Zaheer, M. Sanjabi, A. Talwalkar, and V. Smith, “Federated optimization in heterogeneous networks,” *Proceedings of Machine Learning and Systems*, vol. 2, pp. 429–450, 2020.
- [29] J.-B. Grill, F. Strub, F. Altché, C. Tallec, P. Richemond, E. Buchatskaya, C. Doersch, B. Avila Pires, Z. Guo, M. Gheshlaghi Azar *et al.*, “Bootstrap your own latent: A new approach to self-supervised learning,” *Advances in neural information processing systems*, vol. 33, pp. 21 271–21 284, 2020.
- [30] A. Dosovitskiy, L. Beyer, A. Kolesnikov, D. Weissenborn, X. Zhai, T. Unterthiner, M. Dehghani, M. Minderer, G. Heigold, S. Gelly, J. Uszkoreit, and N. Houlsby, “An image is worth 16x16 words: Transformers for image recognition at scale,” in *International Conference on Learning Representations*, 2021. [Online]. Available: <https://openreview.net/forum?id=YicbFdNTTy>

- [31] P. Goyal, P. Dollár, R. Girshick, P. Noordhuis, L. Wesolowski, A. Kyrola, A. Tulloch, Y. Jia, and K. He, “Accurate, large minibatch sgd: Training imagenet in 1 hour,” *arXiv preprint arXiv:1706.02677*, 2017.
- [32] A. Krizhevsky, “One weird trick for parallelizing convolutional neural networks,” *arXiv preprint arXiv:1404.5997*, 2014.
- [33] A. Coates, A. Ng, and H. Lee, “An analysis of single-layer networks in unsupervised feature learning,” in *Proceedings of the fourteenth international conference on artificial intelligence and statistics*. JMLR Workshop and Conference Proceedings, 2011, pp. 215–223.
- [34] A. Krizhevsky, G. Hinton *et al.*, “Learning multiple layers of features from tiny images,” *Technical report, University of Toronto, 2009*, 2009. [Online]. Available: <https://www.cs.toronto.edu/~kriz/learning-features-2009-TR.pdf>
- [35] Y. Le and X. Yang, “Tiny imagenet visual recognition challenge,” *CS 231N*, vol. 7, no. 7, p. 3, 2015.
- [36] A. Kolesnikov, X. Zhai, and L. Beyer, “Revisiting self-supervised visual representation learning,” in *Proceedings of the IEEE/CVF conference on computer vision and pattern recognition*, 2019, pp. 1920–1929.
- [37] P. Bachman, R. D. Hjelm, and W. Buchwalter, “Learning representations by maximizing mutual information across views,” *Advances in neural information processing systems*, vol. 32, 2019.
- [38] A. Paszke, S. Gross, F. Massa, A. Lerer, J. Bradbury, G. Chanan, T. Killeen, Z. Lin, N. Gimelshein, L. Antiga, A. Desmaison, A. Kopf, E. Yang, Z. DeVito, M. Raison, A. Tejani, S. Chilamkurthy, B. Steiner, L. Fang, J. Bai, and S. Chintala, “PyTorch: An Imperative Style, High-Performance Deep Learning Library,” in *Advances in Neural Information Processing Systems 32*, H. Wallach, H. Larochelle, A. Beygelzimer, F. d’Alché Buc, E. Fox, and R. Garnett, Eds. Curran Associates, Inc., 2019, pp. 8024–8035. [Online]. Available: <http://papers.neurips.cc/paper/9015-pytorch-an-imperative-style-high-performance-deep-learning-library.pdf>
- [39] T. S. Ferguson, “A bayesian analysis of some nonparametric problems,” *The annals of statistics*, pp. 209–230, 1973.
- [40] Lennart, Jsevillamol, M. Hobbhahn, T. Besiroglu, and anson.ho, “Estimating training compute of deep learning models,” <https://www.lesswrong.com/posts/HvqQm6o8KnwxbdmhZ/estimating-training-compute-of-deep-learning-models>, 2022.
- [41] M. Hobbhahn and Jsevillamol, “What’s the backward-forward flop ratio for neural networks?” <https://www.lesswrong.com/posts/fnjKpBoWJXcSDwhZk/what-s-the-backward-forward-flop-ratio-for-neural-networks>, 2021.
- [42] D. Amodei, D. Hernandez, G. Sastry, J. Clark, G. Brockman, and I. Sutskever, “Ai and compute,” <https://openai.com/research/ai-and-compute>, 2018.
- [43] M. Hobbhahn and J. Sevilla, “What’s the backward-forward flop ratio for neural networks?” 2021, accessed: 2023-12-15. [Online]. Available: <https://epochai.org/blog/backward-forward-FLOP-ratio>
- [44] c. v. t. FAIR, “fvcore library,” <https://github.com/facebookresearch/fvcore/>, 2021.